Chemical Engineering and Processing 50 (2011) 1160–1168

Contents lists available at SciVerse ScienceDirect

Chemical Engineering and Processing: Process Intensification

journal homepage: www.elsevier.com/locate/cep

Process intensification of encapsulation of functionalized $CaCO_3$ nanoparticles using ultrasound assisted emulsion polymerization

B.A. Bhanvase[a], D.V. Pinjari[b], P.R. Gogate[b], S.H. Sonawane[a,c], A.B. Pandit[b,*]

[a] Vishwakarma Institute of Technology, 666, Upper Indira Nagar, Pune 411 037, India
[b] Institute of Chemical Technology, N.P. Marg, Matunga, Mumbai 400 019, India
[c] Chemical Technology Dept., North Maharashtra University, Jalgaon 425 001, India

ARTICLE INFO

Article history:
Received 13 June 2011
Received in revised form 20 August 2011
Accepted 4 September 2011
Available online 10 September 2011

Keywords:
$PMMA/CaCO_3$ nanocomposite
Ultrasound
Emulsion polymerization
Semibatch process
Encapsulation

ABSTRACT

The present work deals with the use of intensified processes based on the ultrasonic irradiations for the improvement of the process of encapsulation of inorganic nanoparticles into polymer during nanocomposite synthesis process. The cavitational effects produced due to the use of ultrasonic irradiations have been shown to enhance the dispersion of functional nano-inorganic particles into the monomer during polymerization process. The model system is based on the nanocomposite of poly(methyl methacrylate)/calcium carbonate ($PMMA/CaCO_3$) which has been synthesized by ultrasound assisted semibatch emulsion polymerization. $CaCO_3$ nanoparticles were pretreated with myristic acid in order to improve the compatibility of the monomer with the inorganic particles. TEM image of $PMMA/CaCO_3$ composite particles with well-defined core–shell structure give direct evidence of encapsulation. Effect of encapsulation of $CaCO_3$ particles on thermal properties has been evaluated using thermo-gravimetric methods and it has been observed that the nanocomposites have better thermal stability as compared to the PMMA.

1. Introduction

Inorganic–organic nano-composite materials have gained enormous interest in different applications due to the significant changes that can be obtained in various properties such as mechanical, thermal, electrical, optical and magnetic as compared to the pure polymers [1–8]. The nano-composite can be tailor made for a specific application considering the requirements of the specific class of properties by changing the different synthesis parameters and the suitable combination of the polymer and the additive. Formation of alloy of the inorganic additives and polymers is accomplished by means of surface encapsulation or surface grafting, which needs to be properly controlled, as there is a high chance that the polymer and inorganic particles lead to separation and create discrete phases. Several methods have been implemented to synthesize polymer nano-composite using surface encapsulation such as mini-emulsion polymerization [9], intercalative polymerization [10], solution casting method [11] and hybrid latex polymerization [12]. These approaches mainly produce latex solutions of nanocomposite but in most of the reports the emphasis has been mainly on the synthesis of the composite concentrating on maximizing the yields. The present work concentrates on improvement in the nano-composite latex properties by using the cavitational effects induced using ultrasonic irradiations in the conventional emulsion polymerization approach operated in a semi-batch mode.

Emulsion polymerization is possibly a most convenient way for encapsulation and preparation of polymer/inorganic composite particles [13–15]. In the conventional approach of emulsion polymerization, dispersed monomer droplet acts as nanoreactor for the growth of polymer and also possible agglomeration of the droplets is generally avoided by using a surfactant in the continuous phase. However the addition of inorganic particles during the emulsion polymerization makes the system unstable and leads to agglomeration of the particles. Thus a more versatile approach is needed in the case of encapsulation in order to create homogeneous dispersion of inorganic particles in the polymer matrix. It is very important to state here that the compatibility of the inorganic material with the polymer and the dispersion of nano inorganic filler is very important as these affect the property profile of polymer nanocomposite matrix and hence the suitability for the desired application.

The technique of simultaneous addition of the inorganic particles during the polymer nanocomposite synthesis has not been used generally [15,16] as it has been observed that the nanometer size inorganic particles have a strong tendency for agglomeration because of their high surface energy [17–19]. Surface modification of inorganic particle with an organic molecule is one of the ways to reduce the surface energy and also simultaneously increase the

* Corresponding author. Tel.: +91 22 33612012; fax: +91 22 33611020.
E-mail address: dr.pandit@gmail.com (A.B. Pandit).

0255-2701/$ – see front matter © 2011 Elsevier B.V. All rights reserved.
doi:10.1016/j.cep.2011.09.002

compatibility with the organic polymer matrix [20–24]. The surface modification aspects have been extensively reported in the literature based on the surfactants containing reactive functional groups such as silane coupling agents [25,26], titanate coupling agents [27], stearic acid [28], and myristic acid [29].

The present work also focuses the use of ultrasonic irradiations for improving the dispersion process which controls the effectiveness of the overall encapsulation procedure and the surface properties of the final synthesized product. When ultrasonic waves pass through a liquid medium, large numbers of microbubbles form, grow, and collapse in very short time leading to the cavitational effects of intense turbulence, liquid circulation currents and also formation of the free radicals. In the present case, the collapse of cavitation bubbles near the interface of immiscible liquids will cause disruption of the phases due to the generated microjets and associated turbulence resulting in the formation of very fine emulsions [30]. It is also expected that the problem of agglomeration may be resolved by the use of cavitation during the emulsion polymerization process [31].

The model compound selected in the present work, PMMA, is an important commercial polymer with different applications ranging from aircraft glazing, lighting, dentures, food-handling equipment, contact lenses, etc. [32]. There have been some previous studies dealing with the composite of PMMA and/or $CaCO_3$ as the filler materials. Avella et al. [32] have encapsulated $CaCO_3$ into PMMA by an in situ conventional polymerization process with an objective of improving the abrasion resistance. It has been reported that the obtained nanocomposites by adding only 2% of $CaCO_3$ nanoparticles, showed an average weight loss of about half with respect to that of neat PMMA indicating a significant increase in the resistance. Xie et al. [33] have prepared PVC/$CaCO_3$ composite by conventional in situ polymerization of vinyl chloride in the presence of $CaCO_3$ nanoparticles and reported that $CaCO_3$ nanoparticles were uniformly distributed in the PVC matrix during in situ polymerization of vinyl chloride. Bhanvase and Sonawane [34] have reported the synthesis of polyaniline/$CaCO_3$ nanocomposite using in situ emulsion polymerization in an ultrasonic bath type of reactor. It was observed that ultrasound assisted in situ emulsion polymerization results in a uniform dispersion of nano $CaCO_3$ into polyaniline giving significant improvement in the mechanical and anticorrosive properties. In many conventional in situ polymerization synthesis processes, fine dispersion of nanoparticles in polymer latex is not achieved especially for the increased loading of nanofiller [8,32,35,36]. The use of ultrasonication during in situ emulsion polymerization can improve the dispersion of nanofillers in polymer latex with higher nanofiller loading, which controls the final nanocomposite size. In the present work, PMMA/$CaCO_3$ nano-composite has been prepared by ultrasound assisted semi-batch emulsion polymerization of MMA with added initiator in the presence of functionalized $CaCO_3$ nanoparticles. Calcium carbonate ($CaCO_3$) nanoparticles have been functionalized with myristic acid, in order to improve the compatibility between nanofillers and MMA monomer.

2. Experimental methodology

2.1. Materials

Methyl methacrylate (MMA, density: 0.936 g/cm^3 A.R. grade) was procured from Sigma Aldrich. Surfactant, sodium lauryl sulphate (SLS, $NaC_{12}H_{25}SO_4$) and initiator, potassium persulfate (KPS, $K_2S_2O_8$) have been procured from S.D. Fine Chem. Ltd., Mumbai and have been used as received from the supplier. Myristic acid (MA) coated nano-size $CaCO_3$ was synthesized in the laboratory and was subsequently used for the preparation of PMMA/$CaCO_3$ nano-composite. Deionized water with conductivity of <0.2 μS/cm generated using the Elix 3 UV Water Purification System, has been used throughout the experimentation.

2.2. Surface modification of Nano-$CaCO_3$

Synthesis of nanosize functionalized $CaCO_3$ was carried out by passing CO_2 gas through calcium hydroxide slurry [20,37]. Myristic acid solution was prepared in methanol by keeping methanol to myristic acid ratio as 4:1 by weight. The myristic acid solution was added dropwise into the flask at 60 °C under continuous sonication for 1 h during the carbonation reaction. The solution was centrifuged so as to remove unreacted myristic acid present in the reaction mixture. During carbonation reaction, Ca^{2+} ions react with myristic acid to form a hydrophobic salt of $Ca(C_{13}H_{27}COO)_2$. Thus the synthesized $CaCO_3$ nanoparticles are hydrophobic due to the deposition of $Ca(C_{13}H_{27}COO)_2$ on the surface of $CaCO_3$. The effectiveness of the surface modification of $CaCO_3$ was evaluated by calculating the active ratio of the hydrophobic to hydrophilic particles (discussed later) and contact angle measurement [38]. On flat solid surface, contact angle was measured by sessile drop technique. Initially pellet was prepared using 1 g of $CaCO_3$ and then water droplet was dropped onto the pellet. The contact angle against water on a horizontal surface of a pellet was measured. The percentage active ratio was measured by calculating the ratio of floated product to the overall weight of sample after agitation. It is expected that the higher active ratio of hydrophobic to hydrophilic particles is an indication of better overall hydrophobic properties.

2.3. Synthesis of PMMA/$CaCO_3$ nanocomposite by ultrasound assisted semi-batch in situ polymerization

The reactor (Fig. 1) used for nano-composite synthesis consists of a jacketed glass vessel provided with ultrasonic horn (13 mm diameter made of stainless steel) equipped with a generator (Sonics Vibra-cell, USA) operating at frequency of 22 kHz and rated output power of 750 W. In the work the horn was operated at 50% amplitude yielding a supplied net power of 375 W. The actual power dissipation as measured using calorimetric method was 45.9 W giving an energy transfer efficiency of 12.24%. The polymerization reaction was carried out under nitrogen atmosphere to reduce the contact of the reaction mixture with oxygen. Initially, aqueous solution of sodium lauryl sulphate solution was prepared along with $CaCO_3$ nanoparticles (1–9 wt% of MMA). After subjecting this solution for 10 min irradiation, it was transferred to the reactor. Also an aqueous initiator solution was prepared separately and transferred in the reactor.

Polymerization was carried out by adding 1 ml of MMA monomer in the reactor initially as seed followed by continuous addition of MMA (9 ml) at a constant rate of 0.3 ml/min over a time period of 30 min. The reactor temperature was maintained constant at 65 °C (±1 °C) throughout the experimental run. The complete reaction was carried over a period of 60 min. The product was filtered and then dried in an oven at 120 °C for 2 h. Monomer to polymer conversion was determined by using gravimetric analysis. During the polymerization process, definite quantity of reaction mixture was removed periodically for analysis. These samples were also dried in an oven at 120 °C to remove water and unreacted monomer. Conversion of monomer was calculated at any time t by using the following Eq. (1):

$$\text{Conversion} = \frac{M_5(1 - M_4 - M_3 - M_2)}{M_1} \quad (1)$$

where M_1 = mass of MMA in wet sample, M_2 = mass fraction of surfactant, M_3 = mass fraction of initiator, M_4 = mass fraction of $CaCO_3$, M_5 = mass of dried sample.

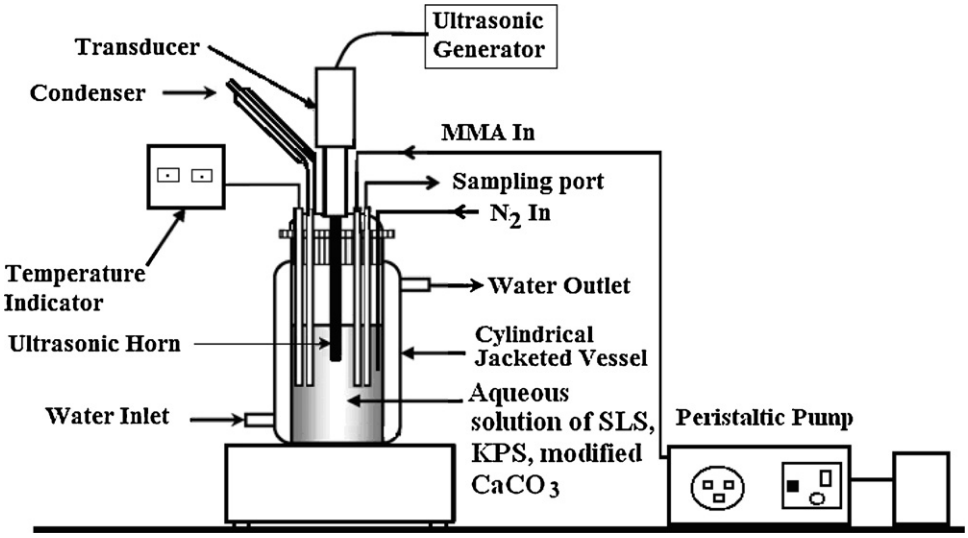

Fig. 1. Schematic representation of the experimental setup for ultrasound assisted PMMA/$CaCO_3$ nanocomposite synthesis.

The total MMA quantity added to the reactor at any time t was calculated by using the following equation (2)

$$M_1 = M_0 + M_t \quad (2)$$

where M_0 = mass of MMA taken at time $t = 0$, M_t = mass of MMA added till the time of sample collection (flow rate multiplied by time of sample withdrawal).

2.4. Characterization

X ray diffraction (XRD) pattern of MA treated $CaCO_3$ and PMMA/$CaCO_3$ nanocomposite was recorded by using powder X-ray diffractometer (Rigaku Mini-Flox, USA). The morphology of PMMA/$CaCO_3$ nanocomposite was investigated by using Scanning Electron Microscopy (SEM) (JEOL JSM, 680LA 15 kV, magnification 10,000×) and Transmission Electron Microscopy (TEM), (PHILIPS, CM200, 20–200 kV, magnification 1,000,000×). Infrared spectroscopic analysis of samples was carried out using SHIMADZU 8400S analyser in the region of 4000–500 cm^{-1}. The composite latex particle size distribution was analysed by Photon Correlation Spectroscopy (PCS, 3000 HAS, analyser Malvern). The weight loss of the MA treated $CaCO_3$, pure PMMA and PMMA/$CaCO_3$ nanocomposite was determined in the rage of room temperature to 800 °C by using a thermogravimetric analysis (PerkinElmer TGA system, USA), at heating rate of 10 °C/min. The contact angle measurement was carried out at 25 °C using a FTÅ 200 (USA) contact angle analyzer. The glass transition temperature (T_g) was measured by Differential Scanning Calorimetry (SHIMADZU DSC–60) in N_2 atmosphere at a heating/cooling rate of 10 °C/min.

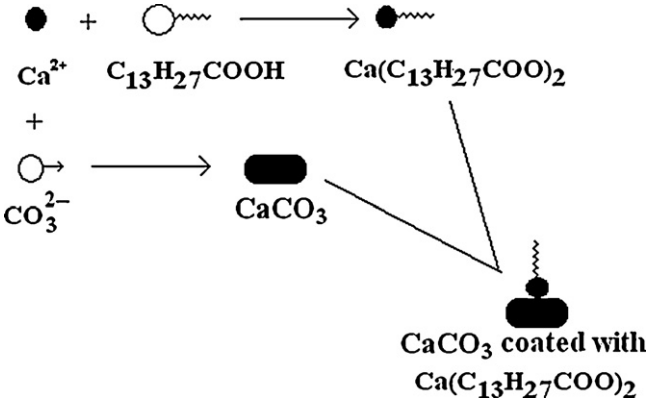

Fig. 2. Schematic representation of the mechanism of the formation of functionalized $CaCO_3$.

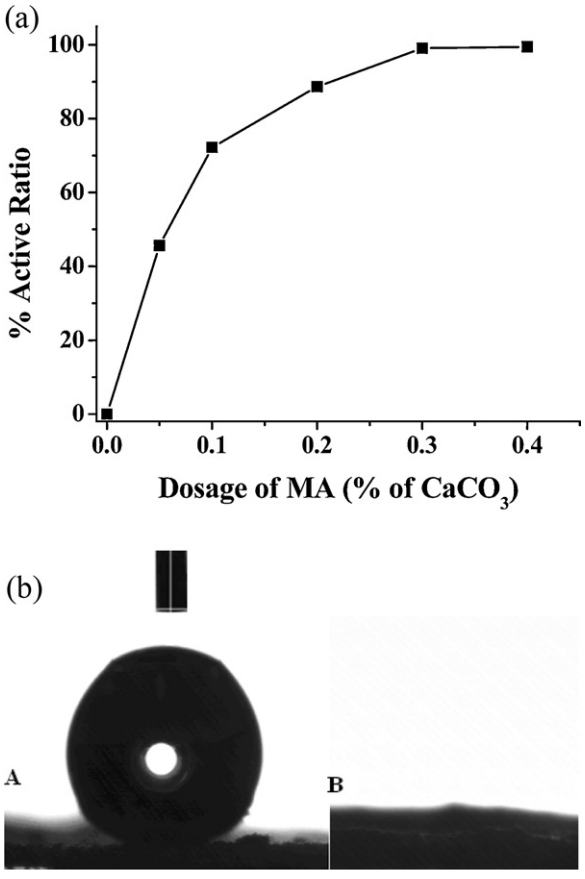

Fig. 3. (a) Influence of dosage of MA on the active ratio of modified $CaCO_3$, (b) the contact angle of (A) modified $CaCO_3$ and (B) untreated $CaCO_3$.

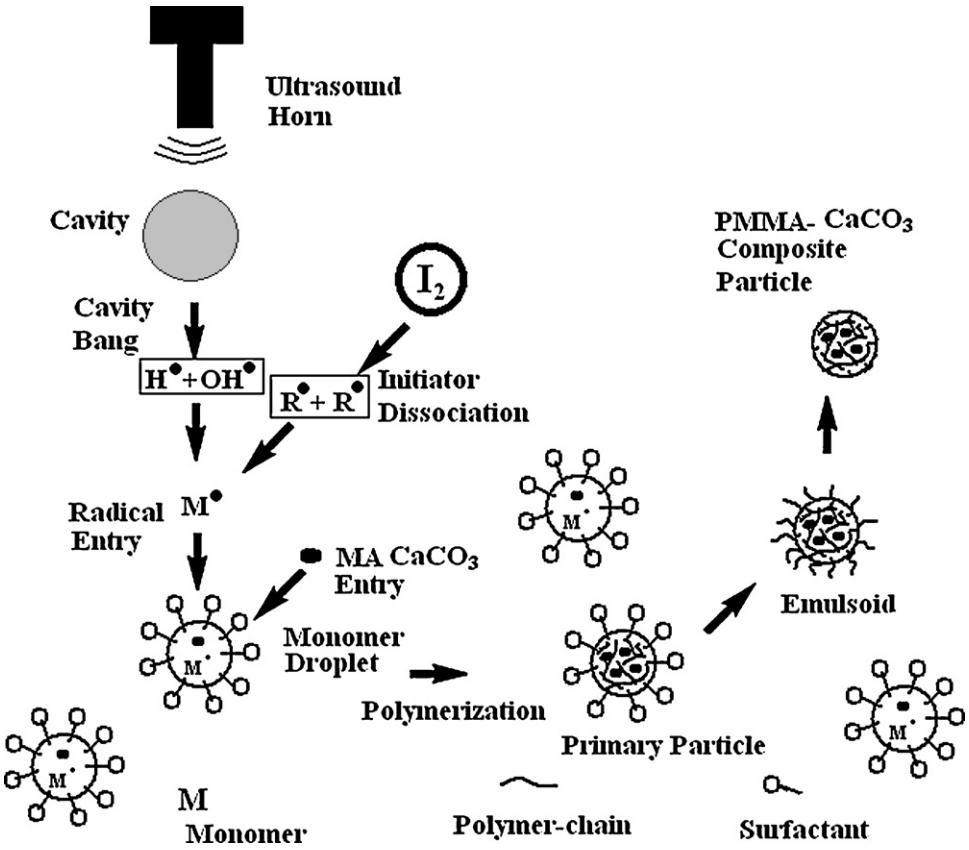

Fig. 4. Schematic mechanism of the formation process of PMMA/$CaCO_3$ nanocomposite.

3. Results and discussion

3.1. Functionalization of $CaCO_3$ nanoparticles

The surface modification of $CaCO_3$ has been achieved using the in situ carbonation process in the presence of ultrasound. The surface modification results in reducing the surface energy of $CaCO_3$ nanoparticles. Myristic acid was also simultaneously added during the synthesis of nano $CaCO_3$ particles. The possible elementary reactions occurring in the carbonation process to give functionalized $CaCO_3$ particles can be given as follows

$$Ca(OH)_2 \rightarrow Ca^{2+} + 2OH^- \quad (3)$$

$$Ca^{2+} + 2C_{13}H_{27}COOH \rightarrow Ca(C_{13}H_{27}COO)_2 + 2H^+ \quad (4)$$

$$CO_2 + H_2O \rightarrow H_2CO_3 \quad (5)$$

$$H_2CO_3 \rightarrow {CO_3}^{2-} + 2H^+ \quad (6)$$

$${CO_3}^{2-} + Ca^{2+} \rightarrow CaCO_3 \quad (7)$$

Initially Ca^{2+} ions react with myristic acid to form a hydrophobic salt of $Ca(C_{13}H_{27}COO)_2$, which acts as a co-surfactant in the reaction mixture and forms $Ca(C_{13}H_{27}COO)_2$, which deposits on the surface of $CaCO_3$. The presence of ultrasonic irradiations helps in reducing the particle size of the final product. The mechanism of the formation of functionalised nanosize $CaCO_3$ has been depicted in Fig. 2.

The hydrophobic properties of the functionalised $CaCO_3$ nanoparticles have been quantified in terms of the active ratio and the contact angle. The dependency of the active ratio, which gives an indication of the hydrophobicity, on the loading of myristic acid has been shown in Fig. 3(a). It can be seen from the figure that with an increase in the dosage of MA from 0.05 to 0.3 wt%, the active ratio improved substantially from 45.6 to 99.1%; however a further increase to 0.4 wt% yielded only a marginal improvement in the active ratio (value of 99.5%). Thus it can be said that for achieving effective hydrophobicity of the $CaCO_3$ nanoparticles, the recommended optimum dosage of myristic acid is 0.3 wt%. The hydrophobic property of modified $CaCO_3$ at 0.3 wt% was also assessed by contact angle measurement (Fig. 3(b)). The contact angle is found to be around 155°, which indicates that particles showed a good hydrophobic property. Also any further increase in the loading of myristic acid only marginally changes the contact angle. Experiments with water drop addition on the untreated $CaCO_3$ indicated that the added water spreads uniformly on the surface of pellet indicating a hydrophilic nature.

3.2. Mechanism of PMMA/$CaCO_3$ nanocomposite formation

The mechanism of the formation of PMMA/$CaCO_3$ nanocomposite by encapsulation has been depicted schematically in Fig. 4. In the initiation stage radicals are generated by dissociation of initiator and water molecules due to the cavitational effects generated by acoustic cavitation. Subsequently in the nucleation stage formation of micelles around MMA droplet takes place. The size of monomer droplet is expected to reduce significantly (possibly to submicron size) due to the turbulence effects of the cavitation during emulsion polymerization. The free radicals enter the monomer droplet resulting into polymerization process. Thus the presence of cavitating effects is expected to improve the nanocomposite formation due to both the chemical effects of formation of free radicals and the physical effects of intense turbulence and liquid circulation currents. It should be noted here that maintaining a proper combination of the operating temperature and ultrasonic power dissipation levels is very important for generation of the adequate

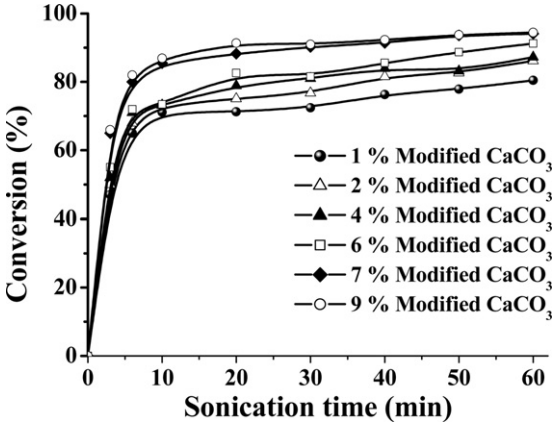

Fig. 5. Effect of percentage $CaCO_3$ loading (of MMA) on conversion (quantity of MMA = 7.2 wt%, quantity of surfactant = 2% of MMA, quantity of initiator = 4% of MMA, temperature = 65 °C).

mixing effects and formation of the required quantities of the free radicals. In a recent work by Dobie and Boodhoo [39], it has been shown that the use of low frequency ultrasound over a power dissipation range of 60–160 W (supplied electric power) does not give the desired degree of beneficial effects at an operating temperature of 45 °C. The quantum of free radicals generated in the system will be dependent on the operating temperature and ultrasonic power dissipation whereas the mixing effects (which are significant at low frequency operation) will be mainly controlled by the ultrasonic power dissipation.

3.3. Effect of $CaCO_3$ loading on the conversion of MMA

The effect of $CaCO_3$ loading on the extent of conversion of MMA was investigated over a concentration range of 1–9% by weight and the obtained results have been shown in Fig. 5. It has been observed that the rate of polymerization increases with an increase in the concentration of the presence of functionalised $CaCO_3$. Similar observations have been reported by Wu et al. [8]. The observed increase in the rates of polymerization can be attributed to the fact that the presence of nanosize calcium carbonate on the interface between monomer and water stabilizes the formed micelles and provide more polymerization sites (nucleating effect of MA coated $CaCO_3$) which in turn enhances the rate of polymerization. Wu et al. [8] have also confirmed the formation of stable emulsions due to the presence of enhanced loading of $CaCO_3$ at the interface.

3.4. Morphology and average particle size of the PMMA/$CaCO_3$ nanocomposites

The TEM images of PMMA/$CaCO_3$ nanocomposite for 4% modified $CaCO_3$ loading have been given in Fig. 6. The 4% modified $CaCO_3$ loading in PMMA latex has been taken as a representative loading which has been observed to give the required alteration in the property profile of the nanocomposite. TEM image of PMMA/$CaCO_3$ nanocomposite confirms the encapsulation of $CaCO_3$ in PMMA matrix. Also, it has been established that the $CaCO_3$ nanoparticles of size 50–100 nm are uniformly dispersed in the polymer latex. Comparison with the earlier work [36], where only conventional approach of in situ emulsion polymerization process was used for encapsulation of $CaCO_3$ nanoparticles, it has been clearly observed that the use of Acoustic cavitation during in situ emulsion polymerization improves the dispersion of modified $CaCO_3$ into PMMA latex compared to conventional in situ emulsion polymerization. Fig. 7(a)–(d) shows SEM micrographs of PMMA/$CaCO_3$ nanocomposite at different loadings of $CaCO_3$. Through the SEM images, it

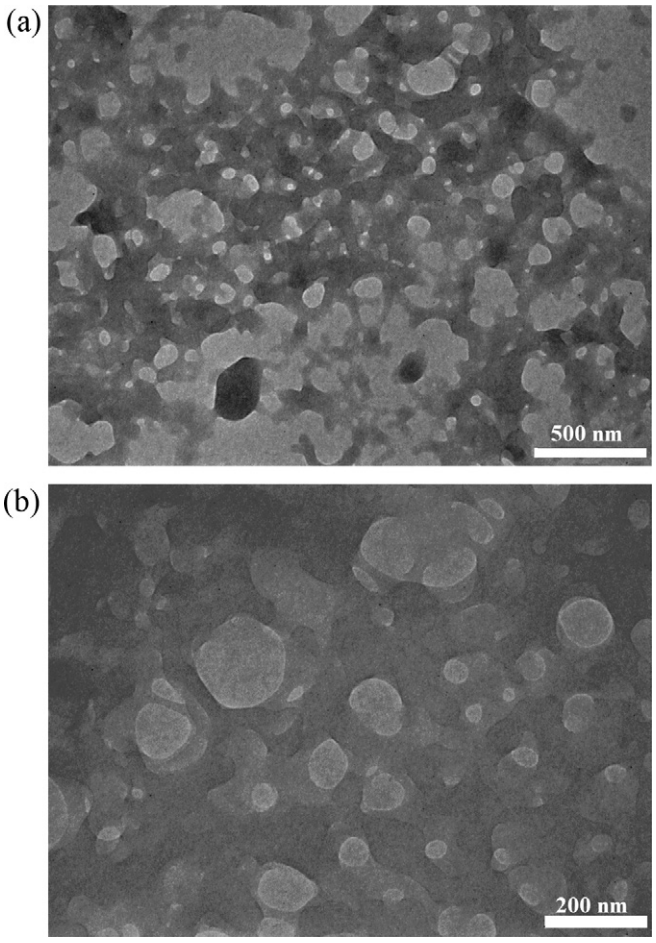

Fig. 6. TEM images of PMMA–4% $CaCO_3$ nanocomposite at (a) 500 nm (b) 200 nm magnification.

is observed that the nanocomposite shows different morphologies and structure with a change in the loading of modified $CaCO_3$. The influence of the loading of $CaCO_3$ on the size of the PMMA/$CaCO_3$ nanocomposite particles, as obtained using Photon Correlation Spectroscopy (PCS), has been given in Table 1. It has been observed that the particle size of PMMA/$CaCO_3$ nanocomposite is in the range of 433–532 nm which is consistent with SEM image (Fig. 7). The size of PMMA/$CaCO_3$ nanocomposite increases with an increase in the modified $CaCO_3$ nanoparticles loading. It may be due to agglomeration effect at higher loading of $CaCO_3$ nanoparticles. Under ultrasonic irradiation, agglomeration of $CaCO_3$ in PMMA/$CaCO_3$ nanocomposite is reduced, but it cannot be completely eliminated. It may be possible to decrease the agglomeration further with ultrasound operated at higher supplied power or by using a larger size probe size as the physical effects of cavitation phenomena will be higher [40].

Table 1
Effect of modified $CaCO_3$ loading on particle size and glass transition temperature (temperature = 65 °C, weight of MMA = 9.36 g, weight of KPS = 0.37 g, weight of SLS = 0.28 g, weight of water = 120 g).

S. No.	% $CaCO_3$ (of MMA)	Particle size (nm) obtained from PCS	Glass transition temperature (°C)
1	0	107	119.5
2	2	433	210.4
3	4	489	210.6
4	6	455	164.5
5	8	484	179.7
6	10	532	182.2

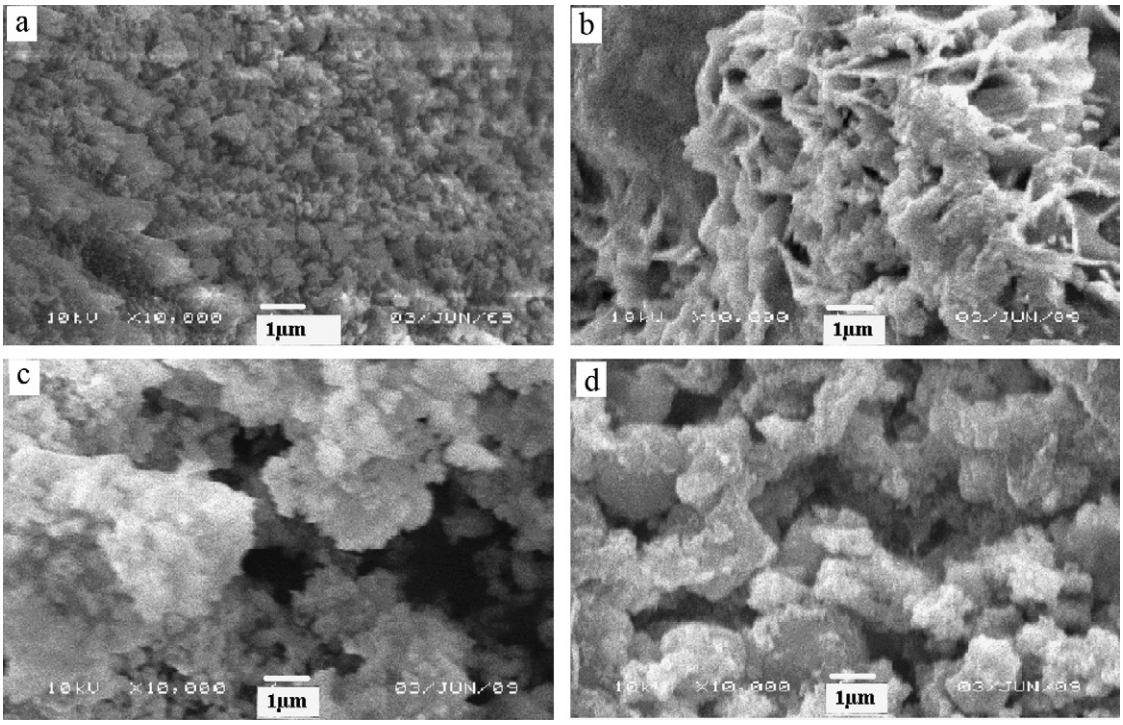

Fig. 7. SEM images of PMMA/$CaCO_3$ nanocomposite at different $CaCO_3$ loading (a) 1% $CaCO_3$, (b) 2% $CaCO_3$, (c) 3% $CaCO_3$, (d) 4% $CaCO_3$.

3.5. XRD analysis of the PMMA/$CaCO_3$ nanocomposites

X ray diffraction analysis was carried out to understand the phase change in the formation of inorganic nanoparticle and nanocomposites. X-ray diffraction (XRD) pattern of MA coated $CaCO_3$ has been shown in Fig. 8(pattern A). The crystallite size of functionalised $CaCO_3$ nanoparticle was estimated as equal to 21 nm by Debye Scherrer's formula, which has been given below for better understanding [37].

$$X_d = \frac{k\lambda}{\beta \cos\theta} \tag{8}$$

where $k = 0.9$, β = full-width at half-maximum height (FWHM) and θ is glancing angle of X rays with the sample holder. CuKα angel $\lambda = 1.5405$ Å radiation was used to obtain XRD patterns.

It has been observed that no change in the calcite phase was observed due to functionalization with myristic acid. Fig. 8(pattern B) illustrates the XRD of PMMA/$CaCO_3$ nanocomposite. The XRD pattern of PMMA/$CaCO_3$ nanocomposite shows the diffraction peaks at 13.48, 29.5, 30.3 and 42.7° (2θ). Above reported peaks at 2θ value confirms the presence of calcite phase of $CaCO_3$. It is also found that the crystallinity of PMMA/$CaCO_3$ nanocomposite increases with the addition of functionalised $CaCO_3$ nanoparticles as indicated by an increase in the values of the intensity of the XRD. The enhanced crystalline nature of PMMA/$CaCO_3$ nanocomposite can be attributed to the fact that the presence of nanosize calcium carbonate provides more polymerization sites (nucleating effect of MA coated $CaCO_3$). The strong interaction between polymer and inorganic phase and local nucleation at many places results in formation of number of small spherolites making the composite more crystalline.

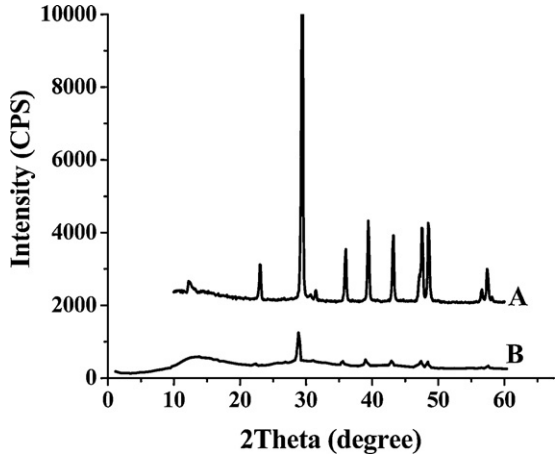

Fig. 8. XRD pattern of (A) modified $CaCO_3$ (B) PMMA-$CaCO_3$ nanocomposite.

3.6. FTIR analysis of the PMMA/$CaCO_3$ nanocomposites

Fig. 9 shows infrared spectra of pure $CaCO_3$, modified $CaCO_3$, Pure PMMA and PMMA/$CaCO_3$ composite particles in the range 4000–400 cm^{-1}. Fig. 9(pattern A and B) shows FTIR spectra of pure $CaCO_3$ and modified $CaCO_3$ nanoparticles respectively. Characteristic peaks of pure $CaCO_3$ nanoparticles are at 1481, 875 and 712 cm^{-1}. In addition to this, peaks at 2918 and 2852 cm^{-1} shows stretching vibration of the C–H which came from the $-CH_3$ and $-CH_2$ in the myristic acid respectively. In this study, the pattern B of Fig. 9 was obtained after the redundant myristic acid was eliminated by rinsing three times with hot methanol. Thus the changed peaks confirm the permanent interaction between the myristic acid and $CaCO_3$ nanoparticles; in other words, the chemical modification of the particles with myristic acid is confirmed by the FTIR analysis. Fig. 9(pattern C) shows a broad band from 1900 to 3000 cm^{-1} due to the presence of C–H stretching vibrations and a sharp intense peak at 1732 cm^{-1} attributed to the presence of C=O stretching vibrations. It also reveals a broad peak ranging from 1000 to 1260 cm^{-1} corresponding to C–O stretching vibrations (ether bond) and a broad band from 650 to 920 cm^{-1} due to C–H bending vibration. As shown in Fig. 9(pattern D) peaks at 1481, 884

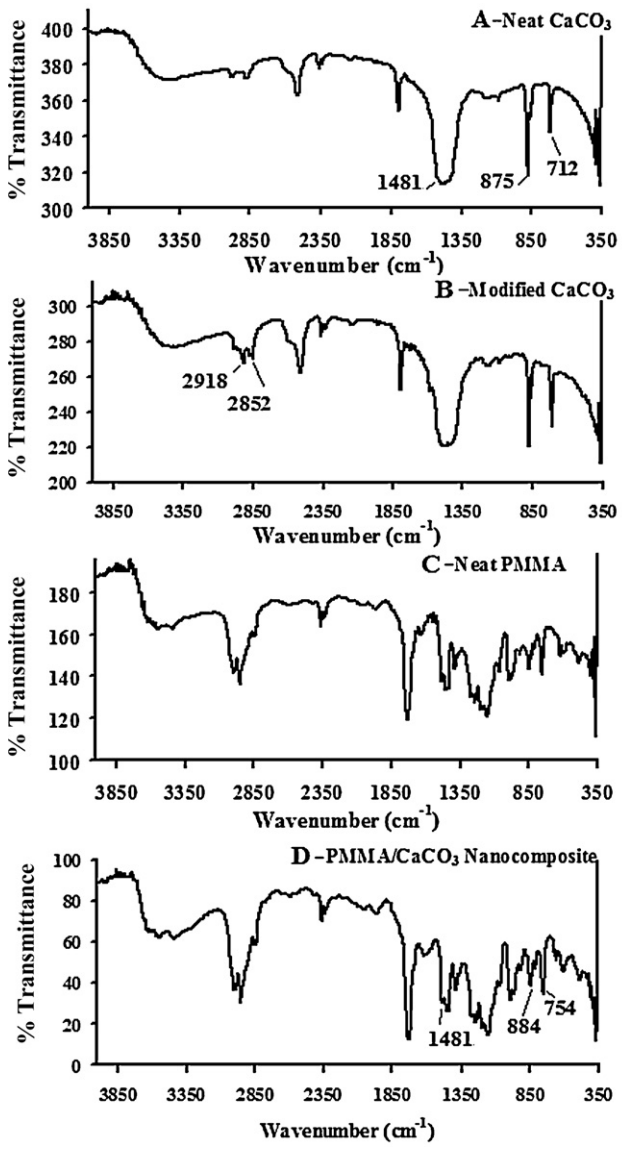

Fig. 9. FTIR spectra showing various bonds in (A) neat $CaCO_3$; (B) modified $CaCO_3$; (C) neat PMMA; (D) PMMA/$CaCO_3$ nanocomposite.

and 754 cm^{-1} indicates the presence of $CaCO_3$ in PMMA/$CaCO_3$ nanocomposite prepared by emulsion polymerization [35,36].

3.7. DSC and thermogravimetric analysis of the PMMA/$CaCO_3$ nanocomposites

Fig. 10 shows thermogravimetric analysis of MA treated $CaCO_3$, pure PMMA, and PMMA–4% $CaCO_3$ composite particles. Fig. 10(pattern A) shows that modified $CaCO_3$ did not decompose below 625 °C and the weight loss of 5% was observed due to decomposition of MA. It is found that the neat PMMA completely decompose in the temperature range of 290–485 °C as shown in Fig. 10(pattern B). The weight loss of PMMA was found at 90.1% at the end of 485 °C. As shown in Fig. 10(pattern C) PMMA/$CaCO_3$ composite shows the weight loss of 83.1% at 475 °C. It was attributed to the decomposition of encapsulating PMMA. In this work, the decomposition temperature of PMMA/$CaCO_3$ composite is found to be higher than that of PMMA. Thus it can be established that the encapsulation of modified $CaCO_3$ nanoparticles could improve the thermal stability of the PMMA matrix. The existence of the $CaCO_3$ in the polymer matrix increases the glass transition temperature (T_g) of the PMMA

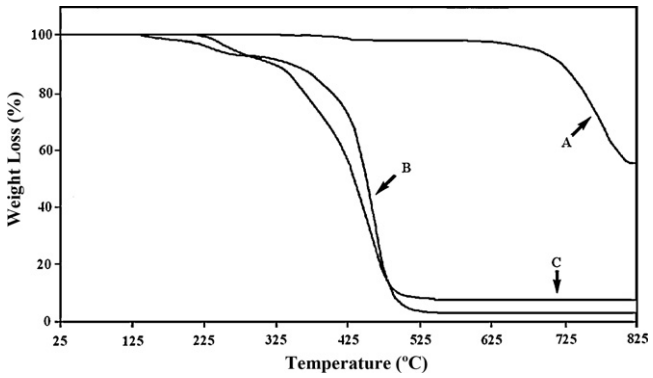

Fig. 10. Thermogravimetric analysis (TGA) plots of (A) modified $CaCO_3$, (B) pure PMMA, (C) PMMA–4% $CaCO_3$ nanocomposite.

composite. DSC results confirm that well dispersed modified $CaCO_3$ nanoparticles restrict the motion of PMMA segmental chains [41]. The glass transition temperature was found to increase from 119.5 (for pure PMMA) to 210.6 °C (at 4% $CaCO_3$ loading) but any further increase in the $CaCO_3$ loading resulted in decreased glass transition temperature (Table 1). The observed decrease can be attributed to the agglomeration effect due to increased loading of modified $CaCO_3$ (from 6 to 9%). This agglomeration weakens the interaction between PMMA chains and modified $CaCO_3$ nanoparticles which leads to decrease in glass transition temperature to 160.5 °C. Under ultrasonic conditions as used in the present work, agglomeration of $CaCO_3$ in PMMA/$CaCO_3$ nanocomposite cannot be completely eliminated but is only reduced to an extent.

3.8. Comparison of the energy efficiency

For the comparison of the energy required for two synthesis methods (conventional in situ emulsion polymerization [36] and ultrasound assisted in situ emulsion polymerization) to obtain PMMA/$CaCO_3$ nanocomposite, a simple calculation has been reported for the optimized conditions in Appendix A. The energy utilized for the synthesis of PMMA/$CaCO_3$ nanocomposite has been calculated as the total energy required (kJ) per unit weight of the material (g) present in the system. The reaction time to synthesize PMMA/$CaCO_3$ nanocomposite was 60 min for ultrasound assisted in situ emulsion polymerization method and 4 h for the conventional in situ emulsion polymerization method. Total energy required per unit weight of the material present in the system is 25.85×10^{-2} kJ/g for ultrasound assisted in situ emulsion polymerization method and 106.35×10^{-2} kJ/g for conventional in situ emulsion polymerization method. Thus, ultrasound assisted in situ emulsion polymerization method has proved to be an energy efficient method which saves more than 75% of energy utilized by conventional in situ emulsion polymerization method along with the reduced in the reaction duration.

4. Conclusions

The present work has clearly established that PMMA/$CaCO_3$ nanocomposites can be successfully synthesized using ultrasound assisted semi-batch emulsion polymerization of methyl methacrylate in the presence of an initiator. $CaCO_3$ nanoparticles can also be effectively modified with different dosage of myristic acid resulting in improved hydrophobic property. Use of cavitation generated due to the ultrasonic irradiations during in situ emulsion polymerization improves the dispersion of modified $CaCO_3$ into PMMA latex compared to conventional in situ emulsion polymerization and also significantly intensifies the process with overall reduction in the

energy requirements. The functionalised $CaCO_3$ were encapsulated in the PMMA due to the good compatibility between the nanofillers and the polymer matrix. The ultrasound based method is effective to increase the loadings of $CaCO_3$ in the composites, which can improve the thermal stability of PMMA/$CaCO_3$ nanocomposites. The results of the thermogravimetric analysis showed the better thermal stability of the nanocomposites than that of PMMA.

Acknowledgement

B.A. Bhanvase acknowledges the BCUD, University of Pune for providing the funding (grant number BCUD/OSD/184/2009) and Indian Academy of Sciences, Bangalore for providing summer research fellowship in 2009. S.H. Sonawane acknowledges Department of Science and Technology Government of India for Fast Track project SR/BY/ET37/2007. Authors are also thankful to Vishwakarma Institute of Technology, Pune for providing the facility to carry out experimental work.

Appendix A. Energy calculations

A.1. Energy delivered during sonication

- Energy delivered during sonication = energy required to synthesize PMMA/$CaCO_3$ nanocomposite.
- Electrical energy delivered during sonication using horn for 10 min (indicated by the power meter) = 4.59 kJ/min.
- Efficiency of horn taken for the calculation = 12.24% (estimated independently using calorimetric studies).
- Actual energy delivered by horn during sonication = energy delivered during sonication using horn in 10 min × total reaction time × Efficiency of horn = 4.59 × 60 × 12.24/100 = 33.71 kJ.
- Quantity of material processed = quantity of water + quantity of MMA + quantity of SDS + quantity of KPS + quantity of $CaCO_3$ = 120 g (120 ml) + 9.36 g + 0.28 g + 0.37 g + 0.37 g (for 4% $CaCO_3$ quantity) = 130.38 g.
- Net energy supplied for processing of material using sonochemical method = actual energy delivered by horn during sonication/quantity of material processed = 33.71 (kJ)/130.38 (g) = 25.85×10^{-2} (kJ/g). (A)

A.2. Energy delivered during conventional method

- Voltage input in magnetic stirrer (Model RQ1210, Remi Metals Gujarat Limited, India) = 230 V.
- Current measured using digital multimeter (KUSAM-MECO Model 2718, Kusam Electrical Industries Ltd., Mumbai, India) = 37 mA = 37×10^{-3} A.
- Power input in overhead stirrer = voltage input × current measured = 230 (V) × 37×10^{-3} (A) = 8.51 W (J/s).
- Time required for completion of reaction = 4 h (14,400 s).
- Net energy delivered during conventional method = power input in magnetic stirrer × time required for completion of reaction = 8.51 J/s × 4 h × 3600 s/h = 122,544 J = 112.544 kJ.
- Energy supplied in form of heat to maintain reaction temperature 75 °C = $mC_{p,mix}$ ($T_{process} - T_{Ref}$) = 130.38 × 4.0058 × (75 − 25) = 26113.81 J = 26.114 kJ.
- Total energy supplied during conventional method = 138.658 kJ.
- Quantity of material processed = quantity of water + quantity of MMA + quantity of SDS + quantity of KPS + quantity of $CaCO_3$ = 120 g (120 ml) + 9.36 g + 0.28 g + 0.37 g + 0.37 g (for 4% $CaCO_3$ quantity) = 130.38 g.
- Net energy supplied for processing of material using conventional method = net energy delivered during conventional method/quantity of material processed = 138.658 (kJ)/130.38 (g) = 106.35×10^{-2} (kJ/g). (B)

A.3. Energy saved

- Net energy saved = (net energy supplied for processing of material using conventional method (B)) − (net energy supplied for processing of material using sonochemical method (A)) = 106.35×10^{-2} (kJ/g) − 25.85×10^{-2} (kJ/g) = 80.50×10^{-2} (kJ/g).

References

[1] R.W. Siegel, Nanostructured materials-mind over matter, Nanostr. Mater. 4 (1994) 121–138.
[2] W. He, C. Pan, T. Lu, Soapless emulsion polymerization of butyl methacrylate through microwave heating, J. Appl. Polym. Sci. 80 (2001) 2455–2459.
[3] Z. Huang, Z. Lin, Z. Cai, K. Mai, Physical and mechanical properties of nano-$CaCO_3$/PP composites modified with acrylic acid, Plast. Rubber Compos. 33 (2004) 343–346.
[4] Y. Lu, J. McLellan, Y. Xia, Synthesis and crystallization of hybrid spherical colloids composed of polystyrene cores and silica shells, Langmuir 20 (2004) 3464–3470.
[5] M. Chen, S. Zhou, B. You, L. Wu, A novel preparation method of raspberrylike PMMA/SiO_2 hybrid microspheres, Macromolecules 38 (2005) 6411–6417.
[6] Z. Li, Y. Zhu, Surface-modification of SiO_2 nanoparticles with oleic acid, Appl. Surf. Sci. 211 (2003) 315–320.
[7] M. Avella, M.E. Errico, S. Martelli, E. Martuscelli, Preparation methodologies of polymer matrix nanocomposites, Appl. Organomet. Chem. 15 (2001) 435–439.
[8] W. Wu, T. He, J. Chen, X. Zhang, Y. Chen, Study on in situ preparation of nano calcium carbonate/PMMA composite particles, Mater. Lett. 60 (2006) 2410–2415.
[9] F. Tiarks, K. Landfester, M. Antonietti, Silica nanoparticles as surfactants and fillers for latexes made by miniemulsion polymerization, Langmuir 17 (2001) 5775–5780.
[10] Y.X. Kong, C. Kan, C. Sun, Encapsulation of calcium carbonate by styrene polymerization, Polym. Adv. Technol. 10 (1999) 54–59.
[11] P. Liu, W.M. Liu, Q.J. Xue, In situ radical transfer addition polymerization of styrene from silica nanoparticles, Eur. Polym. J. 40 (2004) 267–271.
[12] I. Tissot, C. Novat, F. Lefebvre, E. Bourgeat-Lami, Hybrid latex particles coated with silica, Macromolecule 34 (2001) 5737–5739.
[13] X.F. Ma, M. Wang, G. Li, H.Z. Chen, R. Bai, Preparation of polyaniline–TiO_2 composite film with in situ polymerization approach and its gas-sensitivity at room temperature, Mater. Chem. Phys. 98 (2006) 241–247.
[14] B.G. Soares, G.S. Amorim, F.G. Souza, M.G. Oliveira, J.E. Pereira da Silva, The in situ polymerization of aniline in nitrile rubber, Synth. Metals. 156 (2006) 91–98.
[15] D.M. Qi, Y.Z. Bao, Z.X. Weng, Z.M. Huang, Preparation of acrylate polymer/silica nanocomposite particles with high silica encapsulation efficiency via miniemulsion polymerization, Polymer 47 (2006) 4622–4629.
[16] D.M. Qi, Y.Z. Bao, Z.M. Huang, Z.X. Weng, Synthesis and characterization of poly(butyl acrylate)/silica poly(butyl acrylate)/silica/poly(methyl methacrylate) composite particles, J. Appl. Polym. Sci. 99 (2006) 3425–3432.
[17] W.D. Hergeth, P. Starre, K. Schmutzler, Polymerizations in the presence of seeds: 3. Emulsion polymerization of vinyl acetate in the presence of quartz powder, Polymer 29 (1988) 1323–1328.
[18] K. Furasawa, Y. Kimura, T. Tagawa, Syntheses of composite polystyrene latices with silica particles in the core, J. Colloid Interface Sci. 109 (1986) 69–76.
[19] C.H.M. Caris, P.M. Louisa, A.M. Herk, Polymerization of MMA at the surface of inorganic submicron particles, Br. Polym. J. 21 (1989) 133–140.
[20] S.H. Sonawane, P.K. Khanna, S. Meshram, C. Mahajan, M.P. Deosarkar, S. Gumfekar, Combined effect of surfactant and ultrasound on nano calcium carbonate synthesized by crystallization process, Int. J. Chem. Reactor Eng. 7 (2009) A47.
[21] C. Wang, Y. Sheng, X. Zhao, Y. Pan, H. Bala, Z. Wang, Synthesis of hydrophobic $CaCO_3$ nanoparticles, Mater. Lett. 60 (2006) 854–857.
[22] Y. Sh, B. Zhou, C. Wang, X. Zhao, Y. Deng, Z. Wang, In situ preparation of hydrophobic $CaCO_3$ in the presence of sodium oleate, Appl. Surf. Sci. 253 (2006) 1983–1987.
[23] C. Wang, Y. Sheng, H. Bala, X. Zhao, J. Zhao, X. Ma, Z. Wang, A novel aqueous-phase route to synthesize hydrophobic $CaCO_3$ particles in situ, Mater. Sci. Eng. C 27 (2007) 42–45.
[24] S. Mishra, S.H. Sonawane, R.P. Singh, Studies on characterization of nano $CaCO_3$ prepared by in situ deposition technique and its application in PP nanocomposites, J. Polym. Sci., Part B: Polym. Phys. 43 (2005) 107–113.
[25] L.J. Broutman, R.H. Krock, Composite Material, vol. 6, third ed., Academic Press, New York, 1974.
[26] Z. Demjén, B. Pukánszky, E. FÖldes, J. Nagy, Interaction of silane coupling agents with $CaCO_3$, J. Colloid Interface Sci. 190 (1997) 427–436.
[27] S.J. Monte, G. Sugerman, Organo-titanate coupling agents for filled polymer systems, Am. Chem. Soc. Div. Org. Coat. Plast. Chem. Prepr. 36 (1976) 207.

[28] A.G. Xyla, P.G. Koutsoukos, Effect of diphosphonates on the precipitation of calcium carbonate in aqueous solutions, J. Chem. Soc., Faraday Trans 1: Phys. Chem. Cond. Phases 83 (1987) 1477–1484.
[29] G. Nakai, T. Fukuda, K. Hosoi, Surface-coated calcium carbonate particles, method for manufacturing same, and adhesive, U.S. Patent 6,686,044, 2004.
[30] W. Qi, X. Hesheng, Z. Chuhong, Preparation of polymer/inorganic nanoparticles composites through ultrasonic irradiation, J. Appl. Poly. Sci. 80 (2001) 1478–1488.
[31] J.G. Ryu, S.W. Park, H. Kim, J.W. Lee, Power ultrasound effects for in situ compatibilization of polymer–clay nanocomposites, Mater. Sci. Eng. C 24 (2004) 285–288.
[32] M. Avella, M. Errico, E. Martuscelli, Novel PMMA/$CaCO_3$ nanocomposites abrasion resistant prepared by an in situ polymerization process, Nano Lett. 1 (2001) 213–217.
[33] X. Xie, Q. Liu, R. Li, X. Zhou, Q. Zhang, Z. Yu, Y. Mai, Rheological and mechanical properties of PVC/$CaCO_3$ nanocomposites prepared by in situ polymerization, Polymer 45 (2004) 6665–6673.
[34] B.A. Bhanvase, S.H. Sonawane, New approach for simultaneous enhancement of anticorrosive and mechanical properties of coatings: application of water repellent nano $CaCO_3$–PANI emulsion nanocomposite in alkyd resin, Chem. Eng. J. 156 (2010) 177–183.
[35] X. Chen, C. Li, S. Xu, L. Zhang, W. Shao, H.L. Du, Interfacial adhesion and mechanical properties of PMMA-coated $CaCO_3$ nanoparticles reinforced PVC composites, China Particuo. 4 (2006) 25–30.
[36] B.A. Bhanvase, S.P. Gumfekar, S.H. Sonawane, Water-based pmma-nano-$CaCO_3$ nanocomposites by in situ polymerization technique: synthesis, characterization and mechanical properties, Polymer-Plastics Technol. Eng. 48 (2009) 939–944.
[37] S.H. Sonawane, S.R. Shirsath, P.K. Khanna, S. Pawar, C.M. Mahajan, V. Paithankar, V. Shinde, C.V. Kapadnis, An innovative method for effective micro-mixing of CO_2 gas during synthesis of nano-calcite crystal using sonochemical carbonization, Chem. Eng. J. 143 (2008) 308–313.
[38] Y. Sheng, B. Zhou, J.Z. Zhao, N.N. Tao, K.F. Yu, Y.M. Tian, Z.C. Wang, Influence of octadecyl dihydrogen phosphate on the formation of active super-fine calcium carbonate, J. Colloid Interface Sci. 272 (2004) 326–329.
[39] C.G. Dobie, K.V.K. Boodhoo, Surfactant-free emulsion polymerisation of methyl methacrylate and methyl acrylate using intensified processing methods, Chem. Eng. Proc. Process Intensif. 49 (2010) 901–911.
[40] V.S. Sutkar, P.R. Gogate, Design aspects of sonochemical reactors: techniques for understanding cavitational activity distribution and effect of operating parameters, Chem. Eng. J. 155 (2009) 26–36.
[41] J. Zou, Y. Zhao, M. Yang, Y. Dan, Preparation and characterization of poly(MMA-M12-BPMA)/TiO_2 composite particles, Colloid. Polym. Sci. 286 (2008) 1009–1018.